Project No. 2021W-04

Disaster Prevention Research Institute

Kyoto University

Estimation of Bedrock Characteristics Considering Uncertainties of *P*- and *S*-wave velocity structures beneath the Japan Islands Inferred from high-density seismic stations

March 2023

Principle Investigator Mostafa Thabet

DPRI Contact Person Nagashima Fumiaki

Introduction

Robust and systematic evaluation for the bedrock characteristics, such as P- and S-wave velocities and their associated peak resonance frequencies and depths, could contribute significantly to implementing of effective disaster mitigation measures for earthquakes. For this purpose, it is necessary to evaluate the observational (i.e. stable and reliable Horizontal-to-Vertical spectral Ratio of Earthquake, EHVR) and theoretical (i.e. diffuse field inversion) aspects of ground motions and to infer these bedrock characteristics. Consequently, frequency-bedrock depth regression could be established as a direct and powerful tool to explore the bedrock depth, which could be applied in various geophysical and engineering applications.

Thabet (2019 and 2021) could establish new nonlinear regression relationships between bedrock depth (with high impedance contrast) and S-wave resonant frequency using the 698 KiK-net and 1045 K-NET stations. Thus, these previous works are extended by the current collaborative project to improve the applicability and reliability of these relationships through adapting the diffuse field inversion code by Nagashima et al. (2014). We used the diffuse field inversion for tuning the subsurface velocity structure models of the 1743 KiK-net and K-NET stations. A new nonlinear regression relationship is established between bedrock depths and their corresponding S-wave resonant frequencies. Moreover, these tuned models at each station will be used to estimate the engineering and/or seismic bedrocks beneath the Japan Islands.

Methodology

During the first year of the project (FY2021), the procedure to calculate stable and reliable EHVR was set up and examined using several test sites in Japan. This procedure is composed from the following systematic and consecutive steps. First, earthquakes with PGA between 1.0 ~ 50.0 gal are selected and corrected to remove the DC effects. This level of shaking is selected to imply that linear behaviour is prevailing and to avoid later modification due to nonlinear response. Then, the selected earthquakes are grouped based on source distance (*i.e.* $S \leq 50$ km, 50 km $< S <$ 200 km, and $S \geq 200$ km) and source depth (*i.e.* $D \leq 25$ km, 25 km $< D <$ 60 km, and $D \geq 60$ km) to nine groups. Groups A, B, and C has $S \leq 50$ km and $D \leq 25$ km, 25 km $< D <$ 60 km, and $D \geq 60$ km, respectively. Groups D, E, and F has 50 km $< S <$ 200 km and $D \leq 25$ km, 25 km $< D <$ 60 km, and $D \geq 60$ km, respectively. Groups G, H, and I has $S \geq 200$ km and $D \leq 25$ km, 25 km $< D <$ 60 km, and $D \geq 60$ km, respectively. After that, the *S*-waves and surface waves time windows are picked automatically using Kurtosis function applied on these selected and grouped earthquake records. These picked time windows are processed using 5% tapering

and zero padding after the windowed part to make the whole time series length suitable for the consequent Fourier spectra calculation. The calculated Fourier spectra for the EW, NS, and UD components are smoothed using Parzen window function with 0.1 Hz width. Then, the EHVR of each earthquake are calculated. Finally, at each frequency point of the spectra, only EHVR ratios, which have high signal-to-noise ratios (SNR), are geometrically averaged. EHVRs with their corresponding low SNRs are excluded from further calculation due to non-stationary at these frequency points, which may significantly affect the physical meaning of the EHVRs.

During the second year of the project (FY2022), the already set up computational framework in the first year (FY2021) was applied on the whole seismic stations of KiK-net and K-NET. The resultant stable averaged EHVR is inputted in the diffuse field inversion to back-calculate the subsurface velocity structure beneath each station. The diffuse field inversion was repeated ten times to insure the stability of inversion process and the associated subsurface structures. As a result, detailed subsurface velocity structures were retrieved at each station. New nonlinear regression relationship between S-wave resonant frequencies and their corresponding bedrock depths was established.

Results

It is important to note that the present study is not aiming to reproduce the *PS*-loggings at K-NET and/or KiK-net stations. However, although the unrestricted search space assigned in the diffuse field inversion code, we could achieve reasonable convergence between the inverted velocity structures and the *PS*-loggings. Figure 1 shows an example of the inversion results at YMNH08 KiK-net station. This figure indicates that the inversion procedure used can give us stable results and the identified velocity structures correspond to PS-logging data.

Figure 2 shows the established regression between the resonance frequencies (*i.e.* first and second peak frequencies) and the corresponding bedrock depths. The number of stations used to create this regression is 1663 K-NET and KiK-net stations. Exclusion of stations is depending on several conditions such as the availability of enough amount of records more than 10, the high variability of the resultant subsurface structures and the matching of the frequencies between observed and inverted EHVRs.

Figure 3 exhibits a regression between the corresponding bedrock depths and the *S*-wave velocities of the overlying layers above the corresponding bedrock. The detailed inverted subsurface structures could be used for further engineering and exploration applications.

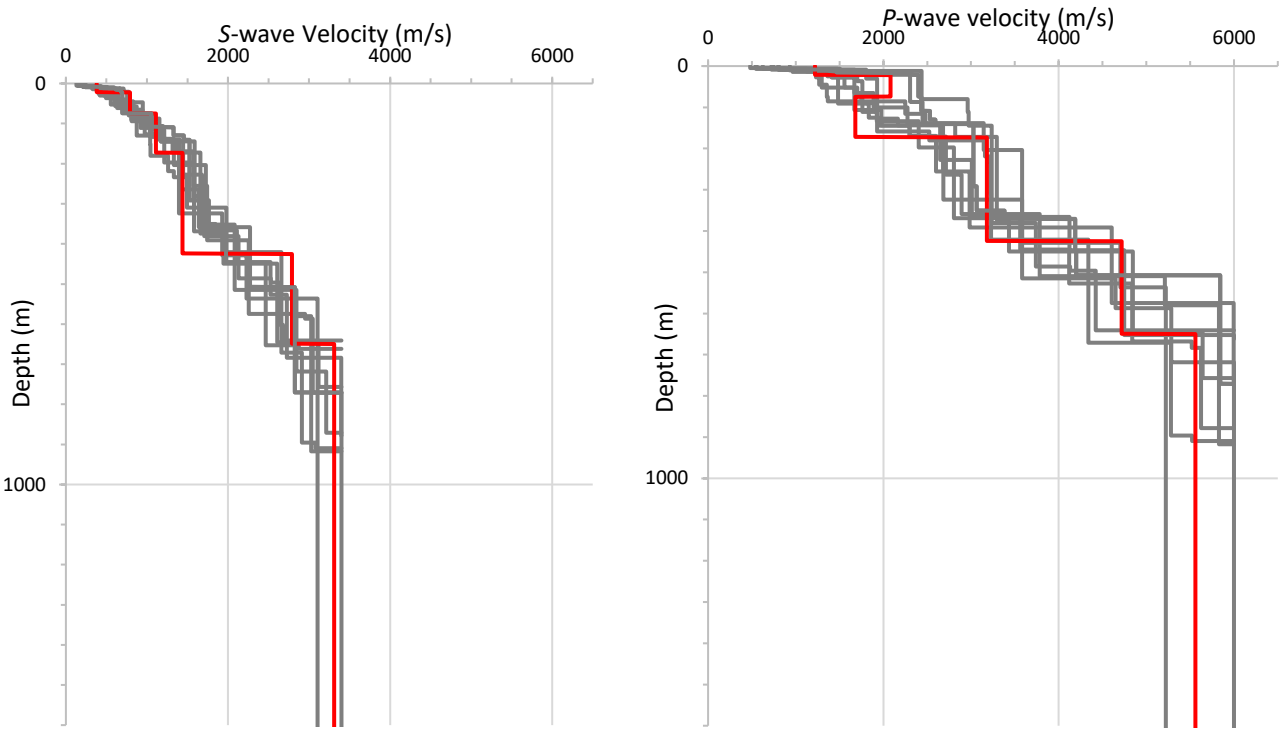

Figure 1. Example diffuse field inverted velocity structures (Gray lines) at YMNH08 station and superimposed with the *PS*-loggings (red line).

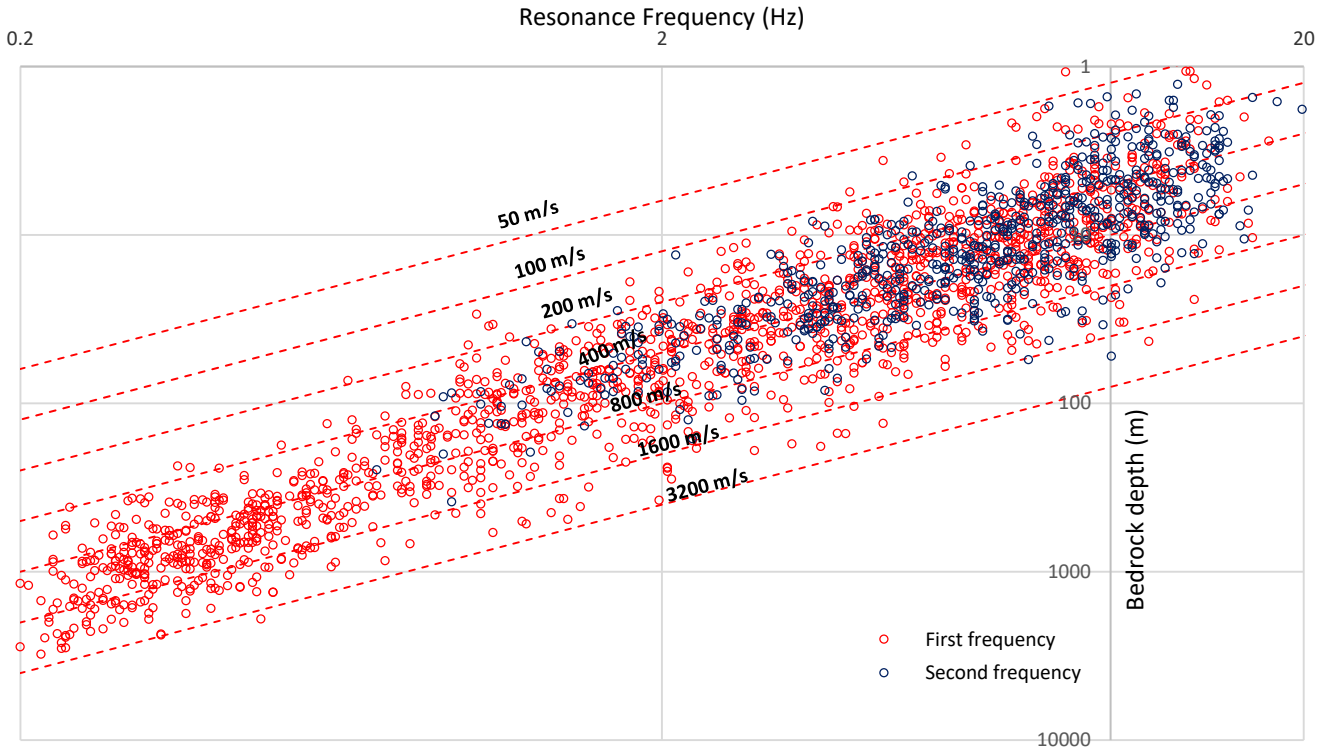

Figure 2. Frequency-bedrock depth regression resulted from diffuse field inverting for EHVRs curves and subsurface structures.

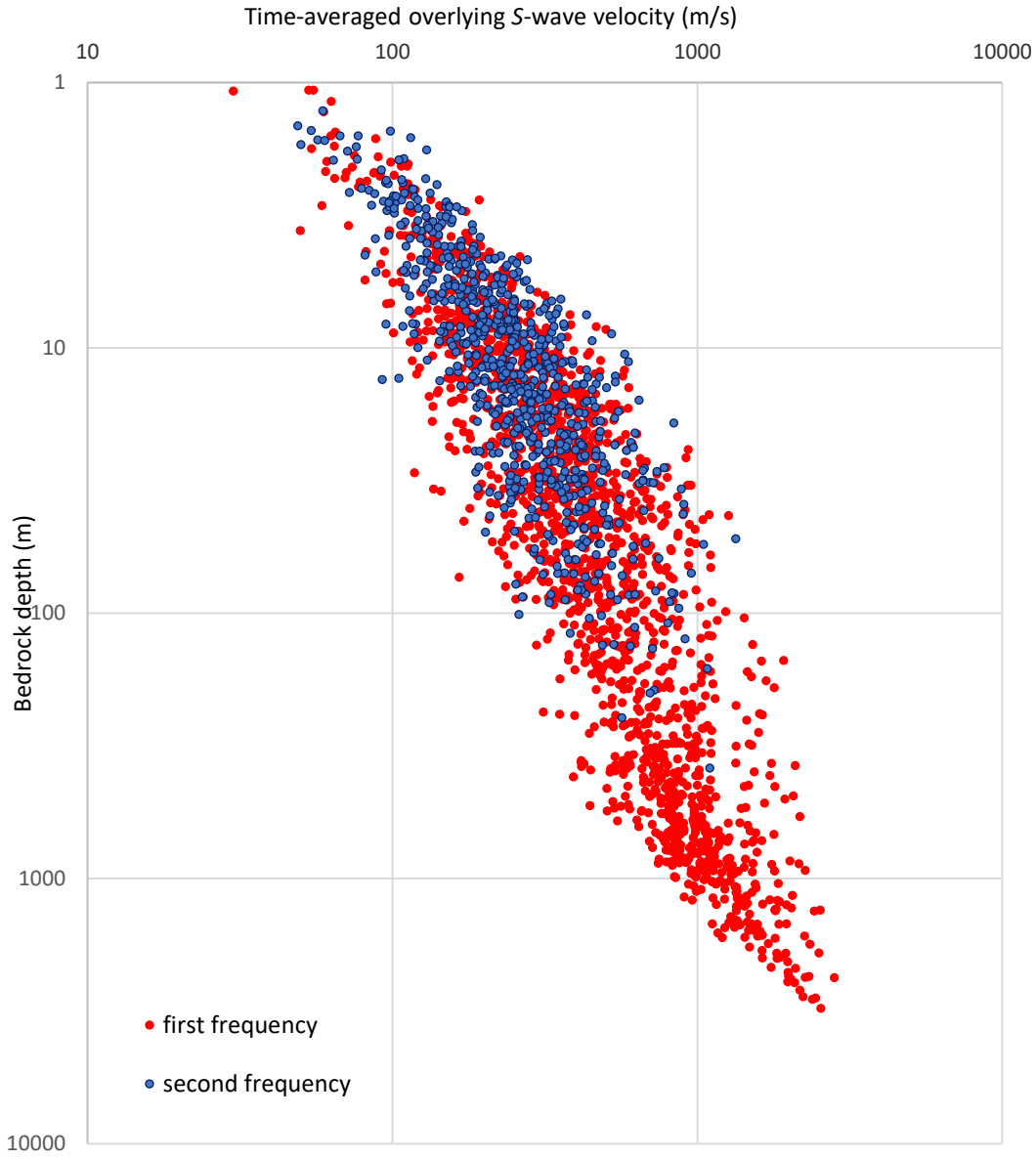

Figure 3. Regression of time-averaged *S*-wave velocity overlying the bedrock versus the bedrock depth.

References

Nagashima, F., S. Matsushima, H. Kawase, F. J. Sánchez-Sesma, T. Hayakawa, T. Satoh, and M. Oshima (2014). Application of horizontal-to-vertical (H/V) spectral ratios of earthquake ground motions to identify subsurface structures at and around the KNET site in Tohoku, Japan, Bull. Seismol. Soc. Am. 104, 2288–2302, doi: 10.1785/0120130219.

Thabet M (2019) Site-specific relationships between bedrock depth and HVSR fundamental resonance frequency using KiK-NET data from Japan. Pure Appl Geophys 176:4809–4831. https:// doi. or g/ 10. 1007/ s00024- 019- 02256-7

Thabet M (2021) Improved site-dependent statistical relationships of VS and resonant frequency versus bedrock depth in Japan. J Seismol 25:1441–1459. https:// doi. org/ 10. 1007/ s10950- 021- 10038-9